

Wrong Before Right: Late Rescue and Interface Failure in Aligned Language Models

Jiaqi Deng
Independent Researcher
djg627@163.com

Abstract

We study how correctness is *assembled* inside aligned language models—not only whether the final answer is right. Using layer-wise difference-in-differences (DiD) trajectories over polarity-controlled minimal pairs, we identify a robust phenomenon we call the **wrong-dip**: in mid layers (25–90% depth), a model’s internal preference transiently commits to the incorrect—often unsafe—answer and is rescued only by late-layer correction. We verify the phenomenon causally with patchscope-style activation transplantation and characterize it across 17 models spanning three families and 64× scale (0.5B–32B). Four findings follow. (1) Alignment amplification of the causal wrong-dip is recipe-specific and emergent: it emerges at 3B in Qwen2.5, remains high, and peaks at 32B ($\Delta\text{dip } +0.140 \rightarrow +0.182$, paired t up to 9.7), reverses significantly in Llama-3-8B ($t = -2.31$), and sits in between for Mistral-7B—the dip audits alignment recipes, not alignment per se. (2) The dip predicts real compression failures with mechanistic specificity: items with large dips on the intact model are 3–7× more likely to flip under genuine late-layer low-rank compression, block dropping, or structured pruning, while flips under quantization are dip-blind—a double dissociation matching the late-rescue mechanism, causally confirmed by selectively ablating late-layer residual contributions. (3) The dip is trainable: a LoRA fine-tune with a mid-layer wrong-margin hinge penalty matches output-only SFT’s perfect held-out accuracy while cutting the causal internal dip by 67–70%, and transfers to compression robustness (mid-SVD retention 0.943 vs 0.872, per-seed McNemar $p = 2.8 \times 10^{-6}/0.013/0.064$); output-only SFT instead worsens the causal dip by up to 2.8× at perfect surface accuracy. (4) Once the readout interface is controlled, the phenomenon survives natural-language I/O: with semantic-candidate readouts, dip stratification of structural-damage failures is significant on naturalistic vignettes ($p = 10^{-3}$ – 10^{-4}), and free-form evaluation fragility separates into a dip-auditable late-rescue layer and a dip-blind interface layer. Together, these results show that output-level correctness can hide a late-rescue production process—and that this process governs structural compression risk, post-training quality, and natural-language evaluation distortion.

1 Introduction

Safety evaluation of language models is dominated by output-level testing. Yet deployment pipelines routinely alter model *internals*—quantization, pruning, low-rank compression, distillation, further fine-tuning. If a model’s correct behavior is maintained by late-layer correction of an internally wrong preference, output-level tests will certify a model whose correctness is one compression step away from failing—and whose apparent competence in natural-language evaluation may reflect interface binding rather than stable internal computation. This paper asks: **do models internally commit to wrong answers before producing right ones; does this matter causally; and can it be measured, predicted, and trained away?**

We give a four-part affirmative answer. Figure 1 previews the account: mid layers transiently prefer the wrong answer; late layers rescue the decision; a readout interface then binds the internal decision to output—and each stage can fail in a measurably different way.

How correctness is assembled: mid-layer wrong → late rescue → readout interface

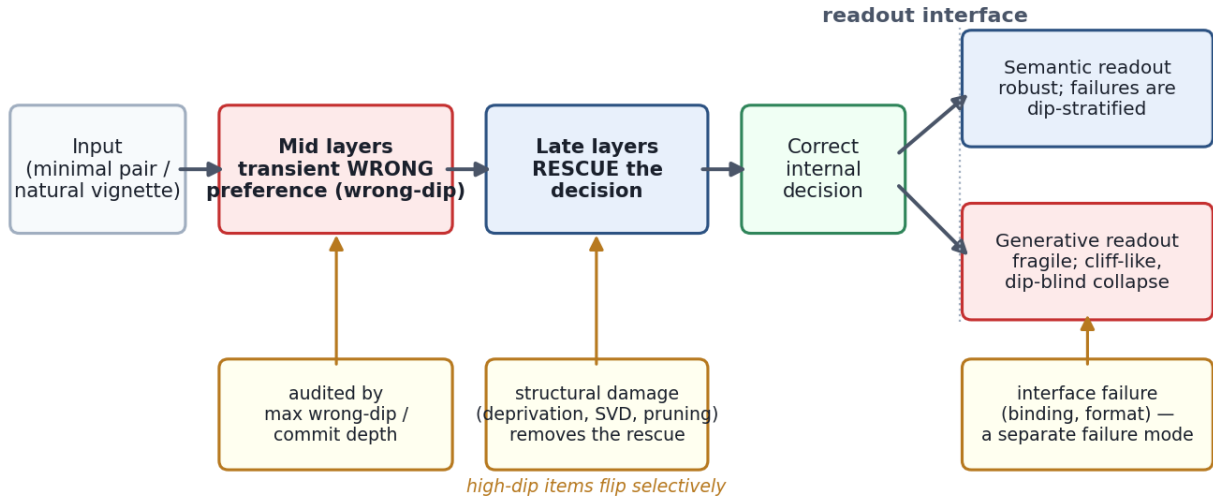


Figure 1: Overview. Mid layers transiently prefer the wrong answer (the wrong-dip, audited by two item-level statistics); late layers rescue the decision; a readout interface then binds the internal decision to output. Structural damage removes the rescue and flips high-dip items selectively (§5); the generative interface fails in a separate, dip-blind way (§5.6).

Phenomenon and metric (§3). On polarity-controlled minimal pairs scored by layer-wise difference-in-differences (DiD), aligned models exhibit a mid-layer excursion toward the *wrong* answer—the **wrong-dip**—that is corrected only near the output. The effect survives tuned-lens re-reading and is verified causally: transplanting mid-layer hidden states into a neutral decoding context makes the model *produce* the wrong answer (patchescopes). We define two item-level statistics, `max_wrong_dip` (depth-windowed maximal wrong-direction excursion) and `commit_layer_frac` (the last depth at which the internal preference disagrees with the output).

Scale and recipe structure (§4). Across a 12-model Qwen2.5 ladder [21] plus Llama-3 [22], Qwen3 and Mistral [23] pairs, instruction tuning *amplifies* the causal dip with a threshold at 3B, sustained amplification thereafter, and a peak at 32B—but the same comparison *reverses* in Llama-3-8B and weakens in Mistral-7B. The dip is a property of the alignment recipe, invisible at the output (accuracy matched $\geq 97\%$ everywhere).

Consequences (§5). The dip, measured on the intact model, predicts *which items* fail under genuine structural compression—late-layer SVD, late block dropping, mid structured pruning—but *not* under quantization, whose failures are diffuse and dip-blind. This double dissociation is exactly what a late-rescue mechanism predicts, and we confirm it causally by attenuating late-layer residual contributions: accuracy barely moves in aggregate, but flips concentrate on high-dip items (up to 29% vs 3%). The phenomenon also generalizes across task families (agent/patient role binding shows 3–6 \times larger causal dips than negation), and—after controlling a readout-interface confound we document in detail—crosses into naturalistic narrative inputs with semantic readouts.

Intervention (§6). A mid-layer wrong-margin hinge penalty added to LoRA SFT (“dip-regularized SFT”) achieves the same perfect held-out accuracy as output-only SFT while reducing the *causal* dip by 67–70%; the fix transfers to structural-compression robustness with per-seed significance at 7B. Output-only SFT, by contrast, worsens the causal dip by up to 2.8 \times while looking perfect at the surface. During training, the

dip separates recipes *after* output accuracy saturates and forecasts final compression retention—a practical training-time monitor, replicated across two scales and two families.

Attribution (§7). A matched-scale family duel links the dip taxonomy to independently reported family differences in low-bit quantization robustness and fine-tuning plasticity: Qwen2.5 learns a forced preference inversion as a late-layer patch; Llama-3 learns it as a mid-layer rewrite.

Contributions. (i) A causally verified account of how correctness is assembled internally, with two cheap item-level metrics; (ii) a scale/recipe map of late rescue and its alignment-specific amplification; (iii) a predictive audit for structural-compression risk with a clean boundary against quantization damage; (iv) a training-level intervention with multi-seed significance, plus evidence that output-only SFT can improve accuracy while worsening internal trajectories; (v) a decomposition of natural-language evaluation failure into late rescue versus interface failure.

2 Related Work

Reading intermediate layers. The logit lens [1] decodes intermediate residual states through the output head; the tuned lens [2] corrects its basis drift with learned affine probes. We use both, and add an out-of-domain-trained tuned lens control to rule out the probe learning away the phenomenon itself. Causal claims rest on activation transplantation in the style of patchscopes [3] and activation patching [4, 5].

Late-layer computation and self-repair. Prior work documents that final layers can overwrite intermediate preferences—“overthinking the truth” in in-context learning [6], and the hydra effect of emergent self-repair when layers are ablated [7]. Layer-pruning studies [8, 9] find deep layers surprisingly removable on average, and LASER [10] shows targeted low-rank reduction can even help. Our contribution is item-level and predictive: we show *which* items depend on late-layer rescue, that this dependence is measurable on the intact model, and that it forecasts failures under structural—but not quantization—damage.

Emergence and scale. Emergent-ability debates [11, 12] concern output-level capabilities. We document an *internal* emergent property: alignment amplification of the causal wrong-dip emerges at 3B in Qwen2.5 and is largest at 32B, while remaining invisible at the output.

Compression and its risks. Post-training quantization [13, 14, 15] and its evaluation on modern families (Qwen3 PTQ study [16]) report family-level robustness differences; compressed models can silently lose safety behaviors [17, 18]. We connect this literature to mechanism: family-level dip differences track *how many* items die under low-bit quantization, while item-level dips predict *which* items die under structural compression.

Training interventions on internals. Representation engineering [19] steers behavior via activation directions; we instead regularize an internal *trajectory shape* during fine-tuning (LoRA [20]) and verify the effect with a causal instrument, avoiding the probe-circularity critique.

3 The Wrong-Dip Phenomenon

3.1 Stimuli

We construct 278 minimal pairs in three categories (value-flip 200, explicit negation 48, permission 30). Each pair ($\text{ctx}_a, \text{ctx}_b$) differs only in a polarity operator, and shares the candidate answer to-

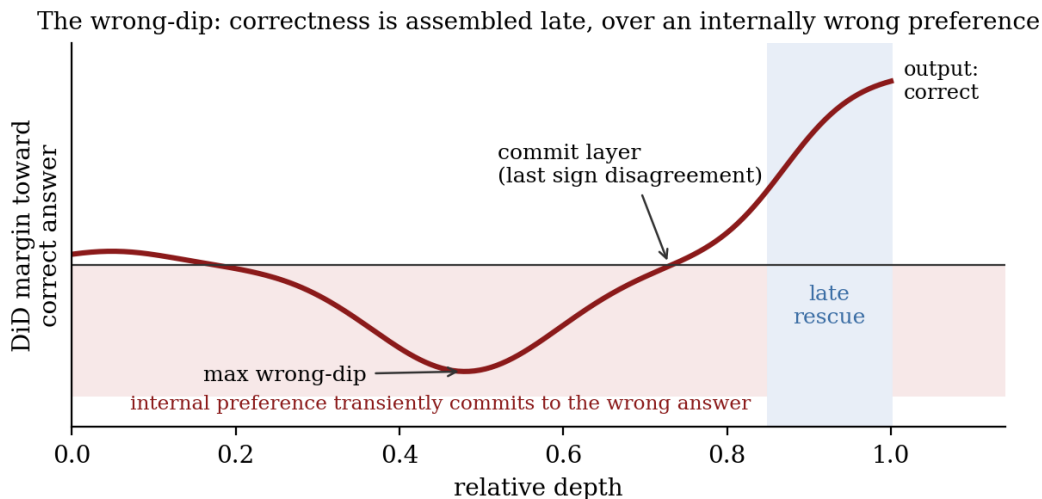


Figure 2: The two item-level statistics on a schematic DiD trajectory: `max_wrong_dip` (deepest wrong-direction excursion in the 25–90% depth window) and `commit_layer_frac` (last depth whose sign disagrees with the output). The final decision is assembled by the late rescue.

kens ($t_{\text{pos}}, t_{\text{neg}}$), which appear symmetrically across contexts (surface control). A safety-relevant subset (harm/law/deception/security/trust) is flagged. A second family of 200 agent/patient role-binding pairs is introduced in §5.4.

3.2 Trajectory metric

For each pair and layer ℓ , $\text{margin}_x(\ell) = \text{logit}_\ell(t_{\text{pos}}) - \text{logit}_\ell(t_{\text{neg}})$, decoded through the final norm and unembedding; $\text{DiD}(\ell) = \text{margin}_a(\ell) - \text{margin}_b(\ell)$. The final-layer DiD is the model’s output decision, so every internal quantity is referenced to the model’s own behavior. We define `max_wrong_dip`—the deepest excursion opposite to the final DiD sign within 25–90% relative depth—and `commit_layer_frac`—the last relative depth whose DiD sign disagrees with the output (Figure 2). The DiD construction cancels item-level lexical frequency and phrasing effects that contaminate raw margins. Measured trajectories are shown in Figure 3.

3.3 Robustness: lens artifacts and causal verification

Three controls address measurement validity. **(i)** An in-domain tuned lens shrinks the dip—but a tuned lens trained on *out-of-domain* general text restores it, indicating the in-domain lens over-corrects by learning the phenomenon itself. **(ii) Causal patchscopes:** transplanting the mid-layer hidden state into a neutral decoding context shows the state *causally drives the wrong token* (full $n = 278$, all 12 ladder models; Figure 4). All cross-family claims in this paper use the causal measure. **(iii)** We document that raw logit lens *overestimates* Llama’s dip (raw 0.72 vs causal 0.023)—a methodological warning for cross-family internal comparisons generally.

4 Scale Emergence and Recipe Reversal

For matched base \leftrightarrow instruct pairs we compute the causal dip difference (instruct – base) with a paired t -test over 278 items (Table 1, Figure 5).

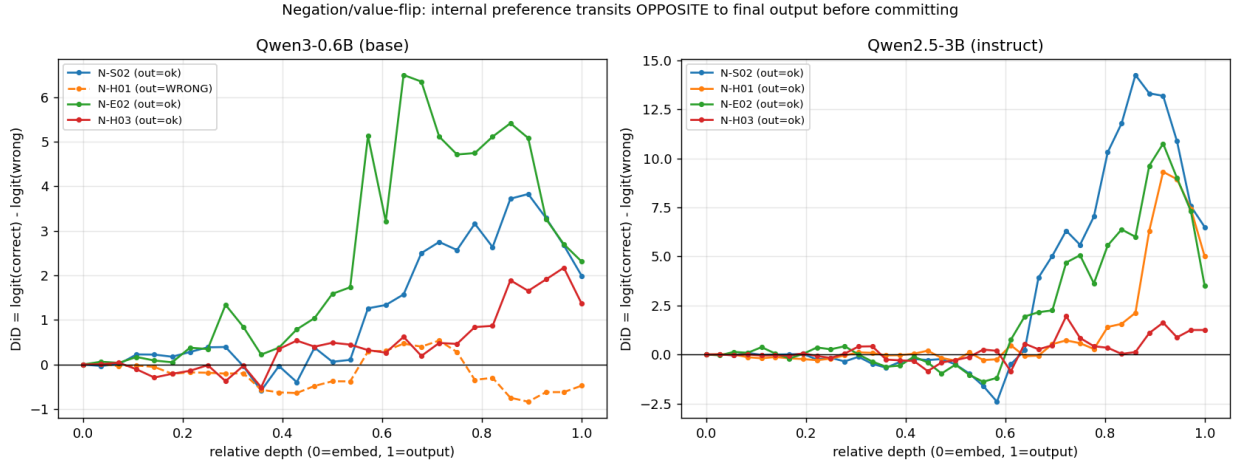


Figure 3: Measured layer-wise DiD trajectories on negation/value-flip minimal pairs. Mid layers transiently prefer the wrong answer before late layers rescue the final decision.

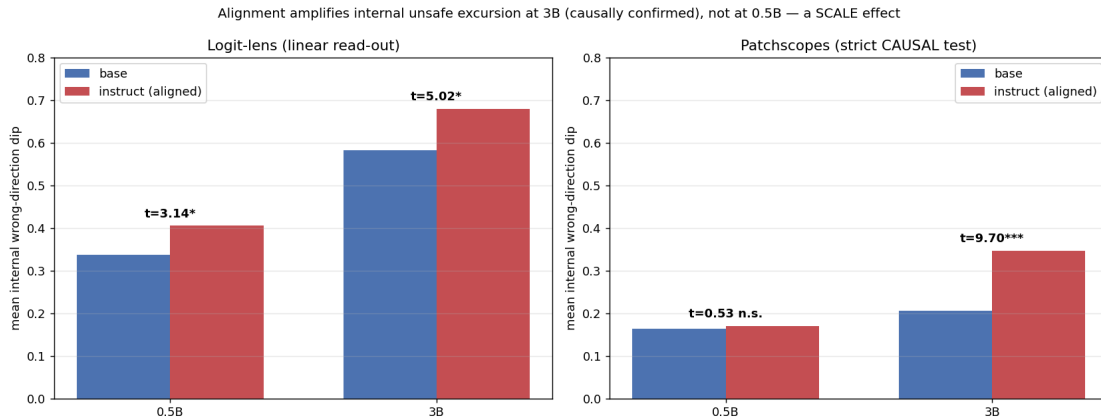


Figure 4: Causal verification. Mid-layer hidden states transplanted into a neutral context drive the wrong token, confirming the dip is carried by the representation itself rather than a lens artifact.

Three observations. **First**, alignment amplification of internal wrongness is *emergent with scale within a recipe*: it emerges at 3B (+0.140), remains high at 7B, and reaches its largest values at 14B/32B—emergence and persistence rather than strict monotonic growth. **Second**, it is *recipe-specific*: Llama-3-8B reverses significantly at comparable scale; Mistral-7B sits between the two styles (weak amplification, shallowest instruct commit depth of all pairs, 0.34)—the taxonomy is a spectrum with three anchored families, not a binary. The same vendor’s next generation, Qwen3-8B, trends in the reversed direction without reaching significance; we report this as *suggestive* cross-generation evidence that the recipe property the dip detects changed between Qwen generations. **Third**, everything above is invisible at the output: pair accuracy is matched ($\geq 97\%$) across all models. Logit-lens commit depth also deepens with scale (32B commit 0.55–0.59; late-binding rate 0.13–0.19, the ladder’s highest): larger models assemble correctness *later* in relative depth.

Table 1: Alignment amplification of the causal wrong-dip across scale and family.

Model	Δ causal dip	paired t	verdict
Qwen2.5-0.5B	+0.007	0.53	null
Qwen2.5-1.5B	+0.013	1.36	null
Qwen2.5-3B	+0.140	9.70	emerges
Qwen2.5-7B	+0.138	7.29	persists
Qwen2.5-14B	+0.169	5.36	rises
Qwen2.5-32B	+0.182	9.37	largest of the ladder
Llama-3-8B	-0.028	-2.31	reverses (significant)
Qwen3-8B	-0.031	-1.29	same-direction trend (n.s.)
Mistral-7B-v0.3	+0.058	+3.10	weak but significant amplification

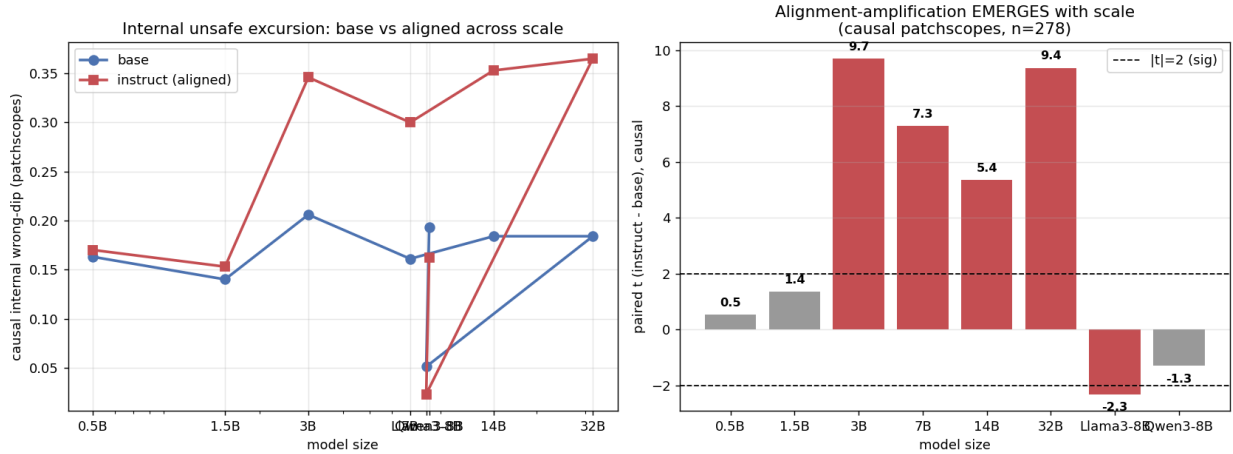


Figure 5: The causal-dip scale ladder. Alignment amplification emerges at 3B in Qwen2.5, remains high, and peaks at 32B; Llama-3-8B reverses; Qwen3-8B trends with Llama. Output accuracy is matched everywhere.

5 What the Dip Predicts—and What It Does Not

5.1 Negative control: the dip does not index surface brittleness

Item-level Spearman correlation between dip and prefix-perturbation flip rate is ≈ 0.08 at 0.5B; the model-level correlation is *negative* (-0.58). Whatever the dip measures, it is not sensitivity to surface prompt noise (12-model sweep).

5.2 Real structural compression: a double dissociation

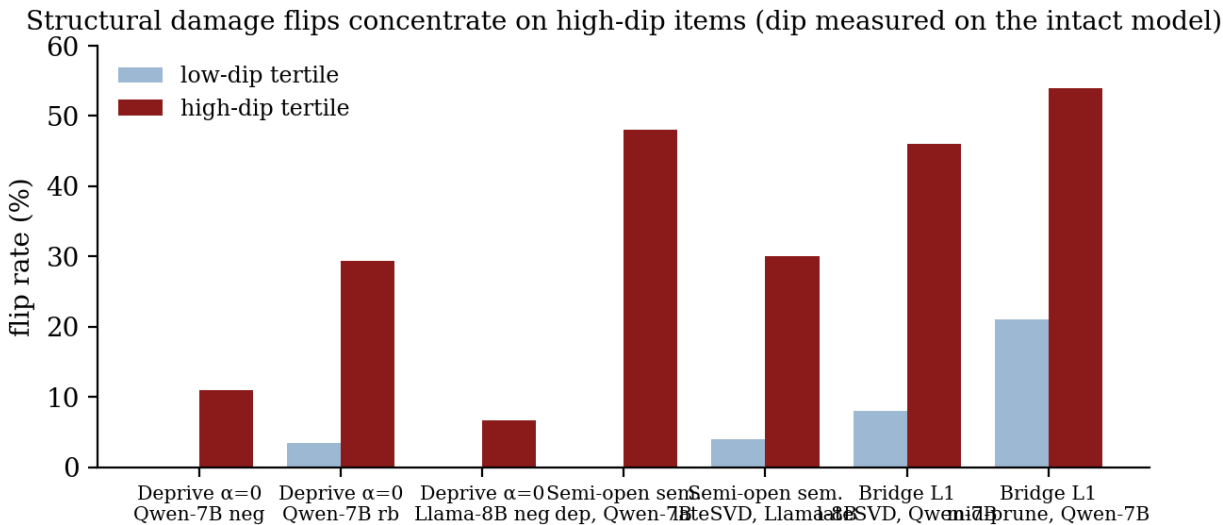
We apply genuine weight-level degradations and score item flips, with the dip always measured on the *intact* model (de-circularized; baseline reload agreement 275–277/278). Table 2 summarizes.

High-dip items are 3–7 \times more likely to flip under **late-layer** low-rank compression; flips under mid-layer compression or whole-depth quantization are not dip-predictable. This is the fingerprint of the late-rescue mechanism: remove the rescuer, and precisely the rescued items fail.

Replication at 7B. In the matched-scale family duel (§7), items dying under late-SVD carry roughly twice the intact dip of survivors (Qwen2.5-7B base 0.99 vs 0.48; instruct 1.24 vs 0.62). By contrast, deaths under

Table 2: Dip-stratification of item flips under real weight-level degradation.

Model	late-MLP SVD (hypothesis)	mid-MLP SVD (control)	int8 whole-depth (control)
Q0.5B base	r128 $p = 0.0016$ (3.7 \times); r64 $p = 0.0038$ (3.0 \times)	$p = 0.14$	$p = 0.78$
Q0.5B instruct	r64 $p = 0.031$ (3.0 \times); r128 $p = 0.081$	$p = 0.16$	$p = 0.65$
Q3B base	r64 $p = 0.035$; dying dip 0.85 vs 0.56 (7 \times)	$p = 0.20$	—

**Figure 6:** Selective failure under structural damage. Across operators (deprivation, late-SVD, mid-pruning), tasks (negation, role binding, semi-open vignettes) and families, items in the high-dip tertile of the *intact* model flip far more often than low-dip items. Statistics in §5.2–5.6.

3-bit RTN quantization are dip-blind (item-level $\rho \approx 0$ in all four models): low-bit damage is diffuse across depth, so no layer-localized signature should—or does—predict it.

5.3 Operator generality: block dropping and structured pruning

To test whether the audit is SVD-specific, we applied two further structural operators to Qwen2.5-7B and Llama-3-8B ($n = 278$): dropping entire late or mid decoder blocks (12.5% of depth, identity replacement) and structured channel pruning (removing the 50% lowest- L_2 -importance MLP intermediate channels). Deaths under **late block-dropping** are strongly dip-marked in both families (dying vs surviving dip 1.22 vs 0.43, MW $p = 0.0003$ in Qwen; 1.94 vs 0.62, $p = 0.003$ in Llama)—the weight-level counterpart of §5.5’s activation-level deprivation. Deaths under **mid structured pruning** are also dip-marked in both ($p = 0.011 / 0.042$). Combined with §5.2 and the dip-blindness of quantization (§6.6), the scope statement is clean: **the dip audits structural damage—low-rank, layer removal, structured pruning; the margin audits quantization** (Figure 6).

5.4 Task generality: role binding

To test negation-specificity we built 200 agent/patient role-binding minimal pairs (surface-symmetric, single-token audited) and reran the full pipeline on Qwen2.5-3B/7B and Llama-3-8B. The wrong-dip is present and *larger* than in negation (causal dip 0.27–0.47 vs 0.16–0.23; commit 0.53–0.64), and the compression double dissociation replicates in all three models (structural deaths dip-marked, e.g. 3B mid-SVD $\rho = +0.33$,

dying 0.97 vs surviving 0.66; quantization deaths dip-blind), with the caveat that item-level ρ at 7B is weaker (+0.07–0.12). Role binding is also far more quantization-fragile than negation (w4 accuracy 0.50–0.70 vs ≥ 0.95). The claim upgrades from a negation finding to a **late-rescue-task finding**; §5.7 pursues what the task family reveals about the core mechanism.

5.5 Causal confirmation: depriving the late rescue

If late layers *rescue* mid-layer errors, attenuating their contribution should expose errors selectively on high-dip items. We scale the residual contribution of the last 15% of decoder blocks by $\alpha \in \{1, 0.5, 0.25, 0\}$, preserving depth and final norm (unlike truncation). Aggregate accuracy barely moves (7B negation 0.98 \rightarrow 0.95 at $\alpha = 0$), but flips concentrate on high-dip items: high- vs low-dip tertile flip rates 11.0% vs 0% (7B negation), **29.3% vs 3.4%** (7B role binding, $\rho = +0.37$), and 6.7% vs 0% in Llama-8B—ordered exactly as the family commit-depth profiles predict. The late-rescue account is thereby causal, not merely correlational.

5.6 From minimal pairs to natural I/O: interface versus mechanism

All results above use minimal pairs with single-token scoring. Bridging to naturalistic I/O produced an instructive four-act sequence.

Act 1: naive bridge (mixed result). We built 96 natural-language DiD pairs (scenario-style value-flip and role-binding vignettes; identical answer options across each pair so the correct label flips; A/B order counterbalanced), answered by free generation with rule-based A/B extraction. Free generation is much harder (clean pair accuracy 0.69 Qwen-7B / 0.54 Llama-8B, from ≥ 0.95 in minimal pairs), and dip stratification of damage-induced flips was directional but non-significant (e.g. 50% vs 36% under full late-deprivation, $p = 0.24$).

Act 2: readout ablation (the interface fails first). The attenuation admits two readings: the mechanism fades in natural settings, or the *readout* does. Re-running the same 96 items under three readouts—free generation (R1), constrained label-token choice (R2), semantic candidates (R3: teacher-forced total logprob of full option phrases, compared at the DiD level to cancel length bias)—favors the interface account on three grounds. (i) Clean accuracy recovers under the semantic readout: Llama-8B 0.542 \rightarrow **0.854**; Qwen-7B 0.688 \rightarrow 0.719. (ii) The internal probe recovers too: semantic-margin dips are $\sim 5\times$ larger than label-token dips (1.15/0.98 vs 0.19/0.22). (iii) With behavior *and* probe both semantic, stratification sharpens to significance: under late-deprivation, high- vs low-semantic-dip tertiles flip at **48% vs 0%** (Qwen-7B, rank-biserial -0.59 , $p = 2 \times 10^{-4}$); under late-SVD, normalized semantic dip stratifies Llama-8B flips at **30% vs 4%** (rb = -0.68 , $p = 9 \times 10^{-4}$). Conversely, *label*-readout deaths concentrate on *low*-semantic-dip items (rb = $+0.75$): label failures are a different failure mode (weak label binding), not the mechanism’s. Wrinkles recorded: Qwen’s late-SVD stratification requires normalization to recover direction ($p = 0.06$); Llama’s deprivation flip base rate under the semantic readout is too low to test (2.4%).

Act 3: the bridge ladder. With the interface identified, we re-tested bridging directly: 96 natural role-binding vignettes (four structural subtypes) under a four-level readout ladder—L1 semantic-candidate logprob, L2 constrained generation, L3 extractive answering, L4 free explanation—each under clean / late-deprivation / late-SVD / mid-pruning, plus prompt-level interface interventions (paraphrase, format schema, verb synonym) as a contrast class. Results (Figure 7): (i) under semantic readout, dip stratification is significant for all three structural operators on Qwen-7B (deprivation rb = -0.99 , $p = 0.018$; late-SVD **46% vs 8%**, $p = 0.0017$; mid-pruning **54% vs 21%**, $p = 0.0019$) and partially replicates on Llama-8B (deprivation $p = 0.034$; late-SVD $p = 0.054$). (ii) Generative readouts are far more fragile: under identical structural damage, L2/L3

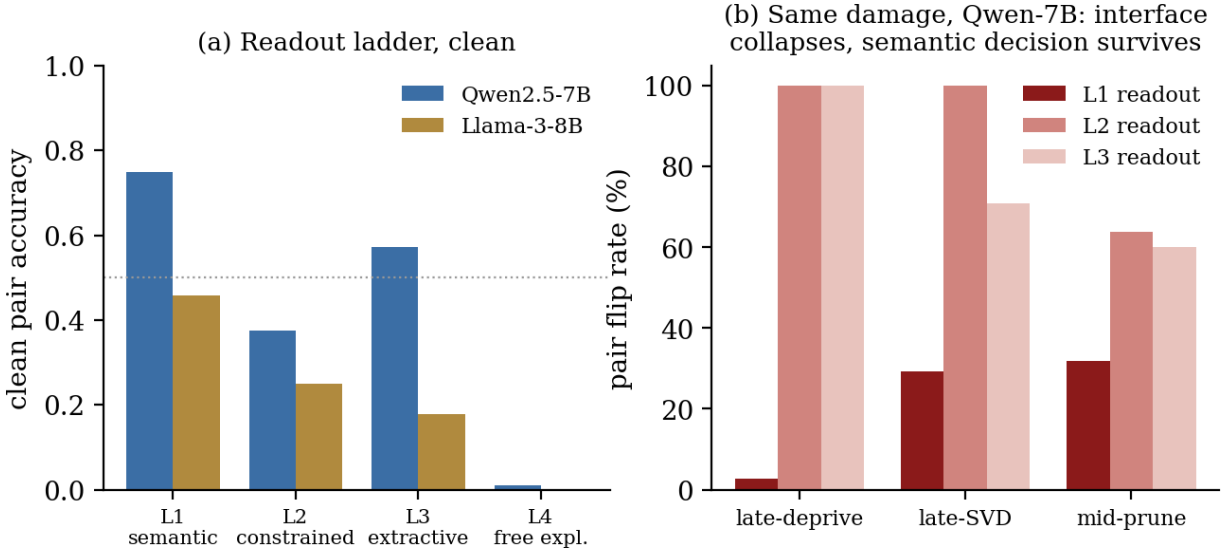


Figure 7: The bridge ladder (§5.6, Act 3). (a) Clean pair accuracy across the four readout levels on natural vignettes: the semantic-candidate decision (L1) is robust; generative readouts degrade stepwise; free explanation (L4) is floored on base models. (b) Under identical structural damage on Qwen-7B, the generative interface collapses (up to 100% flips) while the L1 semantic decision flips far less—and those flips are dip-stratified ($p = 0.0017\text{--}0.019$).

pair flips reach 100% while L1 flips only 3–39%, dip-stratified. (iii) Semi-open degradation therefore combines two separable failures: an internal structural-correction failure that the dip audits, and an answer-interface binding failure that it does not (structural-only flip items exist; interface-only items do not, on base models).

Act 4: the free-generation tier and damage titration. On instruct models with a cross-family independent judge (the other family’s instruct model classifies the generated sentence’s stance), the free-generation pipeline is feasible (clean judged pair accuracy 0.74/0.79). At the damage intensities of Acts 1–3, however, free-generation failure saturates (up to 99% flips—ceiling, untestable). We therefore ran an equal-damage-budget titration with milder grids (late-deprivation $\alpha \in \{0.80, 0.65, 0.50, 0.35\}$; late-SVD $r \in \{512, 256, 128\}$). The titration reveals that the interface’s damage response is cliff-like rather than graded, and family-specific: judged accuracy is barely affected across the whole deprivation grid (0.73–0.85 vs clean 0.74/0.79 for both models—the cliff to 0.09 lies below $\alpha = 0.35$), while under late-SVD Qwen-7B-IT collapses even at the mildest rank (judge 0.04 at r512) but Llama-8B-IT degrades gradually (0.52/0.29/0.19). Consequently, an equal-damage comparison at the free-generation level is only defined on Llama’s graded regime; on Qwen there is no intermediate damage state to titrate to. Free-generation mechanism stratification remains open; the titration shows why—the interface fails abruptly, unlike the graded, dip-stratified semantic layer.

5.7 What is the core? A relational-complexity ladder

Role binding shows 3–6× larger causal dips than negation on the same models (7B: 0.47 vs 0.16; Llama-8B: 0.29 vs 0.05) and deeper commit—suggesting the core phenomenon is *relation assembly under a late-layer correction budget*, with negation its earliest-discovered carrier. A four-tier ladder (single relation / +distractor / two relations / long-distance) partially supports this: the **two-relation tier is a consistent structural-fragility peak** (Llama-8B late-SVD flips 0.62/0.64/**0.90**/0.14 across tiers; mid-pruning 0.19/0.36/**0.53**/0.10; Qwen-7B deprivation also peaks there), and within-ladder dip selectivity replicates (deprivation deaths carry higher dip, $p = 0.010/0.021$; Llama late-SVD $p = 2 \times 10^{-4}$). However, dip/commit do not rise monotonically with

Table 3: Qwen2.5-1.5B (loose split). Dip-regularized SFT matches output accuracy while repairing internals.

arm	acc	dip	commit	fragility	NLL	acc after mid-SVD-r64
base	.965	.487	.479	.139	3.683	.732
official instruct	.979	.558	.475	.144	3.726	.732
output-only SFT	1.00	.652 ↑	.461	.000	3.853	.901
late-only SFT	.979	.504	.477	.050	3.693	.873
dip-reg SFT	1.00	.143	.225	.000	3.725	.979

surface complexity, and the long-distance tier turned out to restate the relation near the query—a design flaw we retired post-hoc as a redundant-cue tier. The honest synthesis: structural fragility tracks *assembly load* (number of bindings simultaneously maintained), not surface complexity, and negation is demoted from mechanism-core to first-discovered instance.

6 Intervention: Structure-Aware Post-Training

6.1 Setup

Qwen2.5-1.5B base (replicated on Llama-3-8B base); LoRA r16; three arms at identical data and budget (~30 s GPU each): **output-only SFT** (all layers, plain CE), **late-quarter SFT** (last 25% of layers only), and **dip-regularized SFT**—CE plus a hinge penalty on wrong-direction logit-lens margins at 30–85% depth. Evaluation is compositionally held out (unseen verbs × unseen frames): train 398 / loose 142 / strict 25 items.

6.2 Main results

Llama-3-8B (loose): dip .716 → .191 (−73%), commit .437 → .243, best NLL of all arms (3.683), mid-compression retention .993; output-only SFT again leaves the dip unrepaired (.676) despite perfect accuracy.

Reading: (i) output-only SFT achieves perfect output accuracy while leaving—or worsening—the internal dip, with the highest capability tax, in both families; (ii) the dip penalty generalizes structurally (internal straightening transfers to held-out lexicon and frames); (iii) late-only tuning is the weakest arm—mid-layer trajectories cannot be repaired from the top.

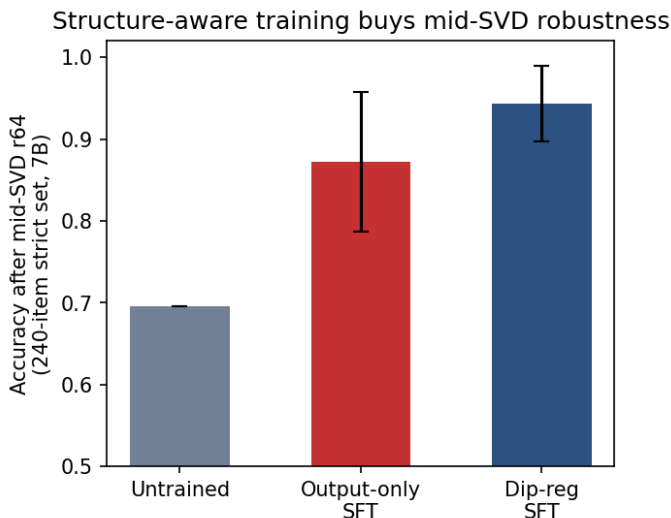
6.3 Robustness transfer at 7B, with significance

We post-train the compression-fragile duel loser (Qwen2.5-7B base) with the same three arms and re-apply the *identical* §7 degradations. Evaluation uses a **240-item strict set** built from entirely new verbs, facts, and frames (zero lexical overlap, audited at generation), **3 seeds** per arm, significance per seed (McNemar within each seed pairing; pooling discordant pairs across seeds would overstate the effective sample size). See Table 4 and Figure 8.

Dip-regularization beats output-only SFT under structural (SVD) compression—+7 points, head-to-head 36:6 / 14:3 / 17:7 across seeds (3/3 same direction, 2/3 individually significant)—precisely where the regularizer acts and the mechanism predicts benefit. Under diffuse 3-bit quantization there is no per-seed signal, mirroring quantization’s dip-blindness (§5.2). Note the division of labor: the audit flags late-SVD-vulnerable items (late-rescue dependence), while the repair straightens mid-layer trajectories and buys mid-SVD robustness. Dip-reg is also lower-variance across seeds ($\pm.046$ vs $\pm.085$).

Table 4: Robustness transfer at 7B (240-item strict set, 3 seeds).

degradation	untrained	output-only SFT	dip-reg SFT	per-seed McNemar p
clean	.967	1.000	.996	—
RTN w4	.887	1.000	1.000	—
RTN w3	.463	.493 ± .035	.528 ± .021	.85 / .50 / .07 (null)
late-SVD r64	.938	.999	1.000	—
mid-SVD r64	.696	.872 ± .085	.943 ± .046	2.8×10^{-6} / .013 / .064

**Figure 8:** Robustness transfer at 7B: dip-regularized SFT retains 0.943 ± 0.046 accuracy after mid-SVD r64 vs 0.872 ± 0.085 for output-only SFT (240-item strict set, 3 seeds).

6.4 Metric-consistency check: causal re-measurement of all trained arms

Because the regularizer optimizes logit-lens margins, lens-measured reductions risk circularity. We re-measured every trained arm with the causal patchscopes instrument (Table 5).

The lens-based conclusions survive—and sharpen—under the causal instrument: dip-regularization reduces the *causal* dip by 67–70% with shallower commit, while output-only SFT makes the causal dip substantially worse in both Qwen models at perfect surface accuracy. Output-only SFT can therefore look successful while degrading the internal trajectory that the dip measures. (Llama’s causal dips are near zero throughout, consistent with its family profile.)

6.5 The dip as a training-time monitor

Training five recipes on Qwen2.5-1.5B (output-only, late-only, dip-reg $\lambda \in \{0.05, 0.2, 0.5\}$) with internal metrics logged every 15 steps: all arms saturate output accuracy by step 30, after which the output cannot distinguish recipes—but the dip keeps separating them, and the end-of-training dip monotonically forecasts final mid-SVD retention (dip 0.66/0.56/0.20/0.08/0.06 → retention 0.887/0.850/0.900/0.975/0.975; dose-response in λ). The signature—output saturates, internals keep diverging—replicates on Qwen2.5-7B and Llama-3-8B (three arms each). The dip→retention forecast holds at both Qwen scales (7B: 0.788 vs 0.925); Llama-8B ceilings the retention scale (output-only SFT already 1.0), consistent with its straight-internals profile—the monitor is most needed exactly where the taxonomy (§7) predicts. Watching the dip during post-training reveals, before any compression test, whether a recipe is improving internals or only the output

Table 5: Causal (patchscopes) dip of all trained arms.

model / arm	untrained	output-only SFT	dip-reg SFT
Qwen2.5-1.5B (loose)	0.129	0.360 (2.8× worse)	0.043 (−67%)
Llama-3-8B (loose)	0.049	0.021	−0.061 (≈0)
Qwen2.5-7B (strict-240)	0.230	0.378 (worse)	0.068 (−70%)

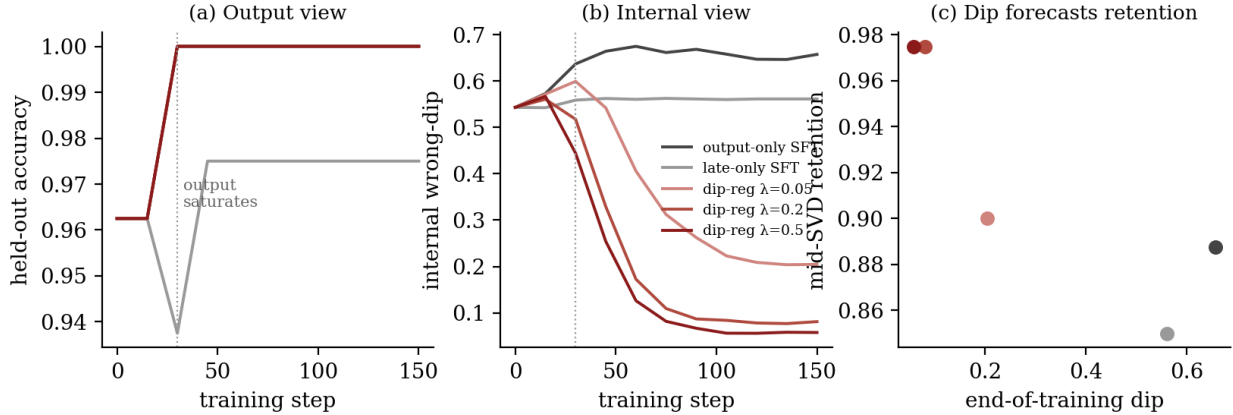


Figure 9: The dip as a training-time monitor (Qwen2.5-1.5B, five recipes). (a) All arms saturate held-out accuracy by step 30—the output view cannot distinguish recipes. (b) The internal dip keeps separating them, with a dose-response in λ . (c) End-of-training dip forecasts final mid-SVD retention. The signature replicates on Qwen2.5-7B and Llama-3-8B.

(Figure 9).

6.6 Toward deployment-grade quantization

With production-style group-wise quantization (bitsandbytes NF4; RTN $g = 128$), 4-bit is near-lossless on our tasks (1–4 deaths per ~ 270) and group-wise w3 survives at 0.87–0.89—most of the per-channel w3 damage in §7 is an artifact of coarse quantization. For predicting the few quantization deaths, a conventional confidence proxy (intact final margin, $\rho \approx -0.30$ to -0.35) *beats* the dip ($\rho \approx +0.06$ to $+0.12$)—fully consistent with quantization dip-blindness. Practical division of labor: **dip audits structural compression (pruning / low-rank / distillation); margin audits quantization.** (AWQ/GPTQ kernels could not be loaded in our environment; we therefore report bitsandbytes-NF4 and group-wise RTN results.)

7 Attribution: Does the Dip Explain Known Family Differences?

External anchors: Llama-3 is more robust than same-size Qwen to ≤ 3 -bit PTQ [16], and shows among the largest fine-tuning gains in low-resource adaptation. Our matched-scale duel (Qwen2.5-7B vs Llama-3-8B, base+instruct; identical RTN w4/w3 and late/mid SVD; $n = 278$):

7.1 Compression duel. At RTN w3 the external result replicates on our task: Llama survives at 0.55/0.59 (base/instruct) vs Qwen 0.46/0.45; at w4 both ≥ 0.95 —the family separation lives entirely at ≤ 3 bits. Under late-SVD both survive ≥ 0.94 , but their *failure anatomies* differ: Qwen’s rare late-SVD deaths are strongly dip-marked; Llama barely dies at all. Item-level mediation shows quantization deaths are dip-blind in both families; but the family-level dip difference (causal dip 0.02 vs 0.30) tracks *how many* die—consistent with late-rescue capacity being the shared resource that low-bit noise exhausts.

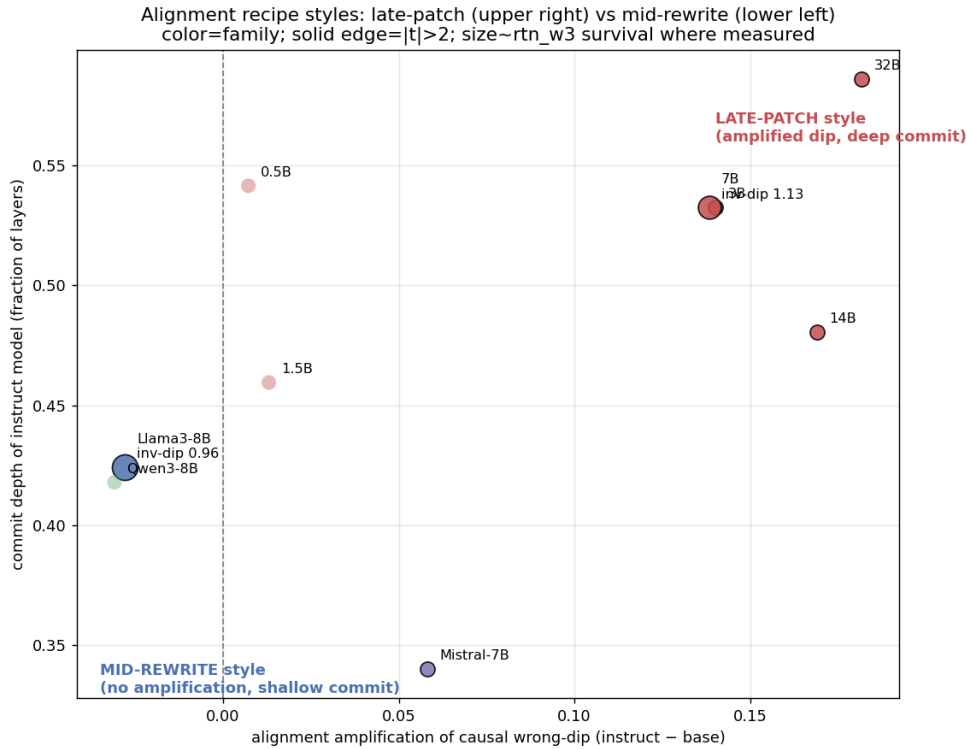


Figure 10: Recipe taxonomy. x : causal alignment amplification (instruct – base); y : instruct commit depth; point size: RTN-w3 survival; annotation: inversion residual dip. Two anchored clusters (late-patch vs mid-rewrite) with Mistral-7B in between.

7.2 Plasticity duel. Both models learn a forced preference inversion to 100% output accuracy in 150 LoRA steps, but by different mechanisms: Qwen-7B carries residual internal dip 1.13 with commit pushed *deeper* (0.64 vs base 0.52)—a **late-layer patch over an intact old preference**—while Llama-8B shows commit *shallower* than base (0.41 vs 0.44)—a **mid-layer rewrite**. Normal SFT shows the same asymmetry in capability tax (NLL 4.07 vs 3.74). Per-layer LoRA delta norms are non-discriminative (~ 0.5 late-half share in both), locating the difference in *function*, not update geometry.

7.3 Recipe taxonomy. Plotting causal alignment amplification against instruct commit depth (point size = w3 survival; annotation = inversion residual dip) separates the models into two anchored clusters—**late-patch** (Qwen2.5 3B–32B) and **mid-rewrite** (Llama-3-8B, Qwen3-8B)—with Mistral-7B in between and the sub-threshold 0.5B/1.5B on the $x \approx 0$ band (Figure 10). The same vendor’s generation change (Qwen2.5→Qwen3) moves the 8B model across clusters, visualizing a suggestive, non-significant cross-generation recipe shift (§4).

8 Discussion

This paper’s central claim is not merely that aligned models can be wrong internally before being right externally. It is that **correctness is assembled**: mid layers often compute a wrong preference, late layers may rescue it, and a separate answer interface may fail even when the internal rescue succeeds. The wrong-dip is our handle on that assembly process.

Mechanistic picture. The results are jointly consistent with a simple account: correct behavior on relation-assembly tasks is produced by mid-layer computation plus a late-layer correction budget. Alignment recipes differ in how much correctness they delegate to the late budget (§4, §7); structural damage—low-rank, layer removal, channel pruning—consumes exactly that budget, so items that lean on it (high dip) fail first (§5); quantization damages diffusely and respects no such item structure; and a training penalty that straightens mid-layer trajectories reduces the delegation, buying structural robustness at zero accuracy cost (§6). The naturalistic experiments add one refinement: on top of this internal layer sits an answer-interface layer whose failure is cliff-like and dip-blind (§5.6)—output-level fragility conflates the two unless the readout is controlled.

Practical guidance. (i) Before compressing an aligned model structurally, run the dip audit on the intact model: it is zero-inference-overhead (one forward pass per item) and flags the items whose correct behavior will fail first. (ii) Before shipping a quantized model, use margin-based confidence instead—the dip is the wrong tool there, and knowing the boundary is part of the contribution. (iii) During post-training, monitor the dip after output accuracy saturates: it forecasts compression retention and distinguishes recipes that repair internals from those that only improve the output. (iv) Cross-family internal comparisons must use causal instruments; raw logit lens can overstate a family’s dip thirty-fold.

9 Limitations

Scope of the evidence. Core evidence rests on two task families of minimal pairs with single-token margin scoring. The naturalistic bridge (§5.6) extends this to narrative inputs and semantic readouts with significant stratification, but fully open-ended dialogue-style external validity remains unestablished: the free-generation tier is feasibility-established, damage titration shows its failure mode is cliff-like and family-dependent, and mechanism stratification at that level remains open. The relational-complexity ladder’s long-distance tier was retired post-hoc for a design flaw (§5.7).

Statistical and training scope. Multi-seed significance is established for the 7B intervention (§6.3) but results elsewhere are single-seed, and training is LoRA-scale only. Capability tax is proxied by corpus NLL; a broader capability battery is future work. Cross-family comparisons are correlational, with causality established only within family via intervention. The Qwen3-8B reversal is a non-significant trend, and quantization-robustness transfer shows no per-seed signal.

Instrumentation. Training-claim internals are verified under causal patchscopes (§6.4), removing the lens-circularity concern. Training-monitor evidence spans two scales and two families with one consequence endpoint (mid-SVD retention), with two caveats: Llama-8B ceilings the retention scale, and at 7B the late-only arm’s retention (0.963) exceeds dip-reg’s (0.925) as a single-point exception. §6.6 evaluates bitsandbytes-NF4 and group-wise RTN rather than AWQ/GPTQ; the §7 result replicates the *direction* of [16] but does not establish the dip as a mediator of quantization failure (item-level quantization deaths are dip-blind).

10 Ethics and Broader Impact

The audit identifies models whose safety behavior is fragile under compression—dual-use exposure is limited since it requires white-box access. Stimuli are restricted to benign objective minimal pairs and naturalistic vignettes; no jailbreak content is used or produced.

Reproducibility Statement

All experiments are scripted end-to-end; every number in this paper maps to a JSON artifact produced by a named script in the accompanying code release. Stimuli: negation/value-flip minimal pairs ($n = 278$), role-binding pairs ($n = 200$), compositional splits (398/142/25), a leakage-audited 240-item strict set, bridge vignettes (96/96), and the relational ladder (256). The release covers the phenomenon pipeline (trajectories, patchscopes), the scale ladder, all compression and structural-damage operators, late-layer deprivation, the training arms with seeds, the causal re-measurement, the training monitor, and the full bridge suite, together with LoRA adapters and a frozen environment specification. A three-tier reproduction package (no-GPU re-analysis; 24 GB single-GPU core results; full 96 GB ladder) accompanies the code. Code, stimuli, and result artifacts will be released at a public repository; the arXiv version will be updated with the link.

References

- [1] nostalgebraist. Interpreting GPT: the logit lens. Blog post, *LessWrong*, 2020. <https://www.lesswrong.com/posts/AcKRB8wDpdaN6v6ru/interpreting-gpt-the-logit-lens>.
- [2] Belrose, N., et al. Eliciting latent predictions from transformers with the tuned lens. *arXiv:2303.08112*, 2023.
- [3] Ghandeharioun, A., et al. Patchscopes: A unifying framework for inspecting hidden representations of language models. *ICML*, 2024.
- [4] Meng, K., et al. Locating and editing factual associations in GPT. *NeurIPS*, 2022.
- [5] Zhang, F., Nanda, N. Towards best practices of activation patching in language models: Metrics and methods. *ICLR*, 2024.
- [6] Halawi, D., et al. Overthinking the truth: Understanding how language models process false demonstrations. *arXiv:2307.09476*, 2023.
- [7] McGrath, T., et al. The hydra effect: Emergent self-repair in language model computations. *arXiv:2307.15771*, 2023.
- [8] Gromov, A., et al. The unreasonable ineffectiveness of the deeper layers. *arXiv:2403.17887*, 2024.
- [9] Men, X., et al. ShortGPT: Layers in large language models are more redundant than you expect. *arXiv:2403.03853*, 2024.
- [10] Sharma, P., Ash, J., Misra, D. The truth is in there: Improving reasoning in language models with layer-selective rank reduction. *ICLR*, 2024.
- [11] Wei, J., et al. Emergent abilities of large language models. *TMLR*, 2022.
- [12] Schaeffer, R., Miranda, B., Koyejo, S. Are emergent abilities of large language models a mirage? *NeurIPS*, 2023.
- [13] Dettmers, T., et al. LLM.int8(): 8-bit matrix multiplication for transformers at scale. *NeurIPS*, 2022.
- [14] Frantar, E., et al. GPTQ: Accurate post-training quantization for generative pre-trained transformers. *ICLR*, 2023.
- [15] Lin, J., et al. AWQ: Activation-aware weight quantization for LLM compression and acceleration. *MLSys*, 2024.
- [16] Zheng, X., Li, Y., Chu, H., Feng, Y., Ma, X., Luo, J., Guo, J., Qin, H., Magno, M., Liu, X. An empirical study of Qwen3 quantization. *arXiv:2505.02214*, 2025.
- [17] Hong, J., et al. Decoding compressed trust: Scrutinizing the trustworthiness of efficient LLMs under compression. *ICML*, 2024.

- [18] Jaiswal, A., et al. Compressing LLMs: The truth is rarely pure and never simple. *ICLR*, 2024.
- [19] Zou, A., et al. Representation engineering: A top-down approach to AI transparency. *arXiv:2310.01405*, 2023.
- [20] Hu, E., et al. LoRA: Low-rank adaptation of large language models. *ICLR*, 2022.
- [21] Yang, A., et al. Qwen2.5 technical report. *arXiv:2412.15115*, 2024.
- [22] Dubey, A., et al. The Llama 3 herd of models. *arXiv:2407.21783*, 2024.
- [23] Jiang, A., et al. Mistral 7B. *arXiv:2310.06825*, 2023.